# Supporting Information

# Donor-acceptor based covalent organic frameworks of nickel(II) porphyrin for selective and efficient $CO_2$ reduction into CO

Nanfeng Xu,[a, b] Yingxue Diao, [c] Xihao Qin, [a] Zhengtao Xu,*[c] Hanzhong Ke*[a] Xunjin Zhu*[b]

[a] Faculty of Materials Science & Chemistry, China University of Geosciences, Wuhan, Hubei 430074, P. R. China. E-mail: kehanz@163.com Tel: (86) 27 67883731

[b] Department of Chemistry, Hong Kong Baptist University, Waterloo Road, Hong Kong, P. R. China. E-mail: xjzhu@hkbu.edu.hk Tel: (852) 3411-5159

[c] Department of Chemistry, City University of Hong Kong, 83 Tat Chee Avenue, Kowloon, Hong Kong, P. R. China.

## Table of Contents

## Experimental sections

### Materials and Instruments

All starting materials and solvents, unless otherwise mentioned, were purchased from commercial sources and used without further purification. Nuclear magnetic resonance (NMR) spectra were recorded on a Bruker Advance III HD (400MHz) spectrometer.

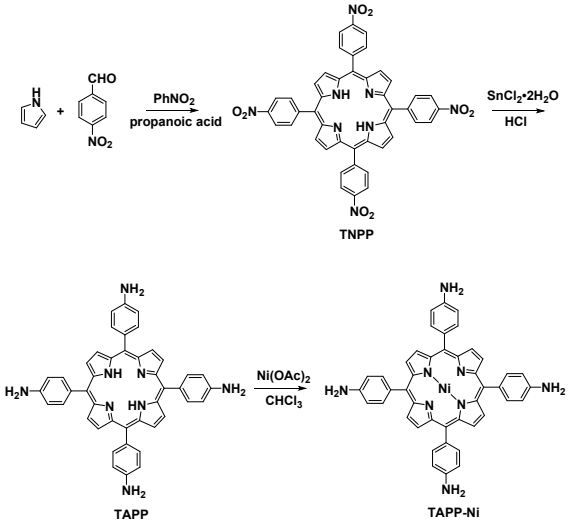


**Scheme S1.** Synthetic route for **TAPP** and **TAPP-Ni**.

**Synthesis of meso-5,10,15,20-tetra-(4-aminophenyl)porphyrin (TAPP): TAPP** used as starting material was synthesized according to the literature.[1] In a 100 mL dried two-neck flask, 4-nitrobenzaldehyde (3.0g, 16.5 mmol) was dissolved in 15 mL nitrobenzene. The mixture was refluxed, and freshly distilled pyrrole (1.2mL, 16.5 mmol) and 4.2 mL propionic acid were added dropwise over a period of 20 min. After refluxed for another 2 h, the resulting solution was cooled to room temperature and 15 mL of methanol was added. The mixture was stirred for 30 min and left

to standing overnight. **The tetra-(4-nitrophenyl)porphyrin (TNPP)** was given by filtration, and washed with methanol and acetone until the eluent present colorless. **TNPP** (220 mg, 2.77 mmol) was dissolved with 10 mL of concentrated hydrochloric acid in a 50 mL dried two-neck flask. Then, $SnCl_2 \cdot 2H_2O$ (0.937g, 41.52mmol) dissolved in 5 mL concentrated hydrochloric acid was dropped within 10.0 min at surrounding temperature. The mixture solution was stirred for 2.5 h and then heated to 65–70 $^oC$ for 30 min. After cooled, the crude products were separated by filtration and scattered in 200 mL water, which was adjusted to pH = 9.00 with concentrated ammonia. The purplish brown solid was obtained by centrifugal separation and dried in a vacuum oven at 30 $^o$ C. The purplish brown solid was purified by Soxhlet extractor with acetone as solvent and column chromatography on Silica eluted with $CHCl_3$ and acetone (V/V=10:1) to get **TAPP** as a purple solid (150 mg). $^1H$ MNR (400 MHz, $CDCl_3$) δ: 8.835 (s, 8H), 7.816 (d, J = 8.0Hz, 8H), 6.967 (d, J=8.0Hz, 8H), 4.007 (s, 8H), -2.733(s, 2H); MALDI-TOF ($C_{44}H_{34}N_8^+$) theoretical value 674.2901, found 674.2943.

**Synthesis of meso-5,10,15,20-tetra-(4-aminophenyl)porphyrinatoNi(II) (TAPP-Ni):** Under a nitrogen atmosphere, **TAPP** (50 mg, 0.047mmol) and nickel acetate (135.94 mg, 0.74mmol) were refluxed in 30 mL $CHCl_3$ for 12h. The solution diluted with 30 mL of $CHCl_3$ and washed with water. The solvent was removed at

reduced pressure and the residue was chromatographed $Al_2O_3$ column to give **TAPP-Ni** as green solid (49 mg). $^1$H MNR (400 MHz, DMSO) δ: 8.750 (s, 8H), 7.625 (d, J = 7.2Hz, 8H), 6.915 (d, J=7.6Hz, 8H), 5.555 (s, 8H); MALDI-TOF ($C_{44}H_{32}N_8Ni^+$) theoretical value 730.2056, found 730.2098.

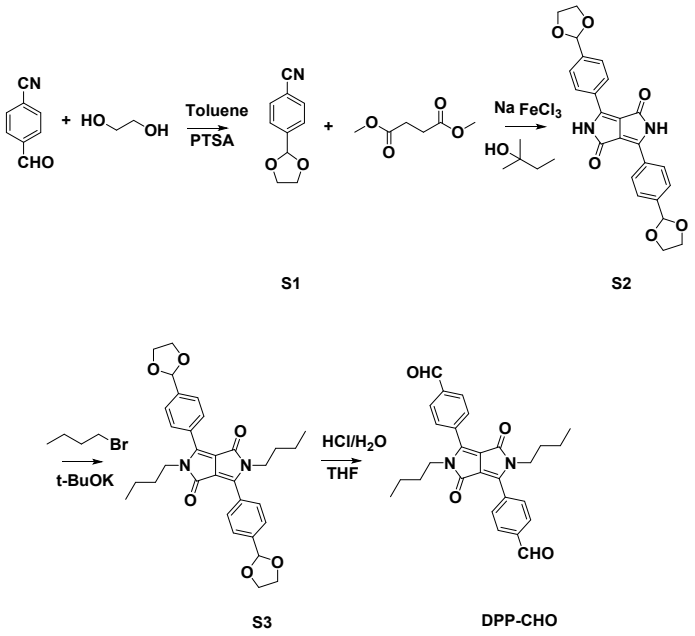


**Scheme S2.** Synthetic route for **DPP-CHO**.

**Synthesis of 4-(1,3-dioxolan-2-yl)benzonitrile (S1):** Ethylene glycol (31 mL, 0.576 mol) and *p*-toluene sulfonic acid (0.013 g, 0.072 mmol) were added into a solution of 4-cyanobenzaldehyde (15 g, 0.114 mol) in 150 mL of toluene. The reaction mixture was refluxed for 12h and a Dean-Stark trap was used to remove generated water during the reaction. After cooled to room temperature, 40 mL of a 5% $NaHCO_3$ aqueous solution was added. The organic layer was extracted with DCM, washed with water three times, and dried over $Na_2SO_4$. The solvent was removed under reduced pressure

to yield **4-(1,3-dioxolan-2-yl)benzonitrile** as a white crystalline solid (17 g, 85%); $^1$H NMR (400 MHz, $CDCl_3$) δ: 7.691 (d, J = 8.0, 2 H,), 7.601 (d, J = 8.4, 2 H), 5.847 (s, 1 H), 4.130-4.040 (m, 4 H).

**Synthesis of 3,6-Bis[4-(1,3-dioxolan-2-yl)phenyl]pyrrolo[3,4-c]pyrrole-1,4-dione (S2):** Under $N_2$ atmosphere, sodium (2.20 g, 96.0 mmol), $FeCl_3$ (0.10 g), and dry *t*-amyl alcohol (48 mL) were mixed. The mixture was heated to 100 °C until the sodium was dissolved completely. Then 4-(1,3-dioxolan-2-yl)benzonitrile ( 8.40 g, 48 mmol) was added. A solution of dimethyl succinate (2.80 g, 19.2 mmol) in dry tert-amyl alcohol (20 mL) was added dropwise during 1 h at 100°C. The solution was stirred for another 24 h at 100 °C, acetic acid (10 mL) was added. After the mixture was allowed to stand for 1h, the precipitate was filtered and washed with hot water and hot methanol until the filtrate was colorless. **3,6-Bis[4-(1,3-dioxolan-2-yl)phenyl]pyrrolo[3,4-c]pyrrole-1,4-dione** was obtained after dried under vacuum (5.70 g, 55%); MALDI-TOF ($[C_{24}H_{20}N_2O_6 + Na]^+$) theoretical value 455.1213, found 455.1220.

**Synthesis of 2,5-Dibutyl-3,6-bis[4-(1,3-dioxolan-2-yl)phenyl] pyrrolo-[3,4-c]pyrrole-1,4-dione (S3):** A mixture of **3,6-Bis[4-(1,3-dioxolan-2-yl)phenyl]pyrrolo[3,4-c]pyrrole-1,4-dione** (4.2 g, 9.7 mmol), potassium tert-butoxide (2.33 g, 20.76 mmol), and dry DMF (120 mL) was heated to 60 °C, 1-bromobutane (9.8 g, 71.6 mmol) in DMF (30 mL) was added slowly, and the mixture was stirred at 60 °C for 12 h. After cooled to room

temperature, dichloromethane (DCM) was added, and then the mixture was washed with water. The organic layer was dried with anhydrous $Na_2SO_4$, and the solvent was removed under reduced pressure. The product was purified by column chromatography with DCM and ethylacetate (V/V = 10/1) as eluent to give **2,5-Dibutyl-3,6-bis[4-(1,3-dioxolan-2-yl)phenyl]pyrrolo-[3,4-c]pyrrole-1,4-dione** as an orange solid (1.05 g, 22 %); $^1$H NMR (400 MHz, $CDCl_3$) δ: 7.829 (d, 4 H, J = 8.4 Hz), 7.645 (d, 4 H, J = 8.0 Hz), 5.879 (s, 2 H), 4.157−4.046 (m, 8 H), 3.746 (t, 4 H, J = 7.6 Hz), 1.575−1.510 (m, 4 H), 1.283−1.208 (m, 4 H), 0.847 (t, 6 H, J = 7.2 Hz).

**Synthesis of 2,5-Dibutyl-3,6-bis(4-formylphenyl)-pyrrolo[3,4-c]pyrrole-1,4-dione (DPP-CHO):** Under $N_2$ atmosphere, **2,5-Dibutyl-3,6-bis[4-(1,3-dioxolan-2-yl)phenyl]pyrrolo-[3,4-c]pyrrole-1,4-dione** (1.0 g, 1.8 mmol) was dissolved in a mixture of THF (20 mL) and HCl (2 M, 10 mL) and the reaction mixture was stirred at 60 °C for 2 h. After cooled to room temperature, DCM (50 mL) was added, and the mixture was washed with water. The organic layer was dried with anhydrous $Na_2SO_4$ and the solvent was removed under reduced pressure. The crude product was purified by column chromatography with DCM and ethylacetate (V/V = 10/1) as eluent to give **2,5-Dibutyl-3,6-bis(4-formylphenyl)-pyrrolo[3,4-c]pyrrole-1,4-dione(DPP-CHO)** as a dark red powder (0.625 g, 75 %); $^1$H NMR (400 MHz, $CDCl_3$) δ: 10.091 (s, 2

H), 8.054 (d, 4 H, J = 8.4 Hz), 7.986 (d, 4 H, J = 8.4 Hz), 3.784 (t, 4 H, J = 7.6 Hz), 1.569−1.511 (m, 4 H), 1.277−1.221 (m, 4 H), 0.850 (t, 6 H, J = 7.2 Hz); MALDI-TOF ($C_{28}H_{28}N_2O_4^+$) theoretical value 456.204, found 456.2009.

**Fourier-transform infrared spectroscopy**

Fourier-transform infrared (FT-IR) spectra of PD-COF-23 and PD-COF-23-Ni were recorded on Nicolet iS50 (Perkin Elmer Paragon 1000 PC) under ambition conditions.

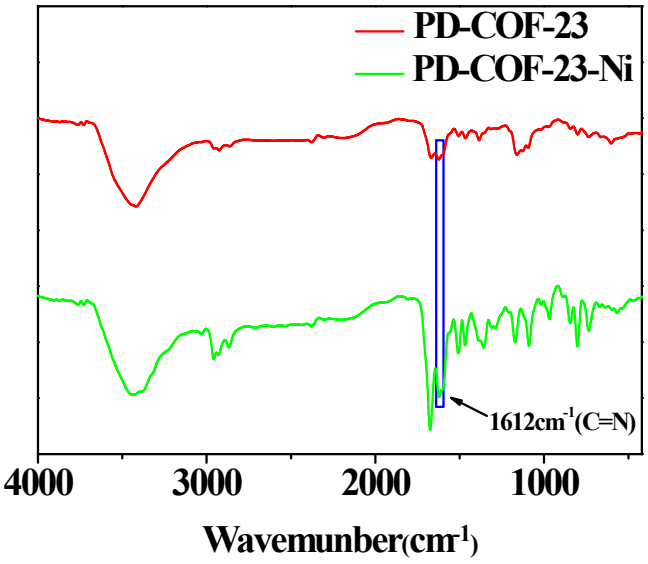


**Figure S1.** FT-IR spectra for PD-COF-23 (red) and PD-COF-23-Ni (green)

**Solid-state nuclear magnetic resonance spectroscopy**

$^{13}C$ CP/MAS solid-state nuclear magnetic resonance (SSNMR) spectra were obtained on Bruker Advance III HD (400MHz) spectrometer.

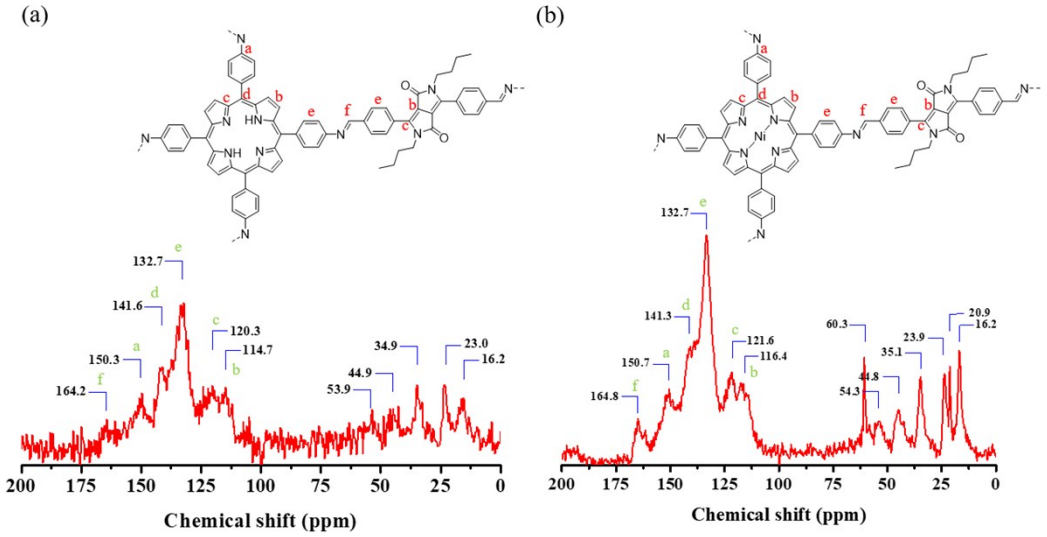


**Figure S2.** $^{13}$C CP-MAS solid-state NMR spectrum of PD-COF-23 (a) and PD-COF-23-Ni (b)

## X-ray photoelectron spectroscopy

X-ray photoelectron spectroscopy (XPS) were carried out on an Sengyang SKL-12 electron spectrometer with VG CLAM 4 MCD electron energy analyzer under Al Kα radiation (1496.3 eV) at a current of 15 mA and 10 kV.

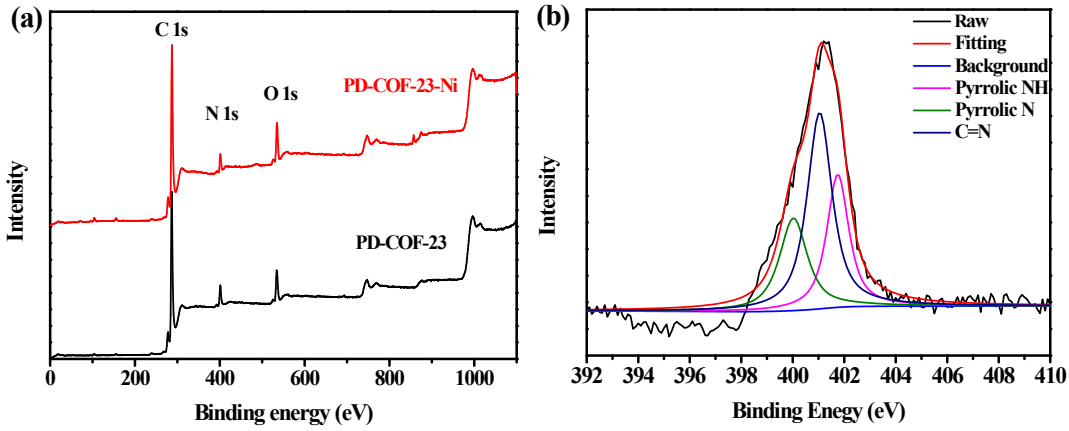

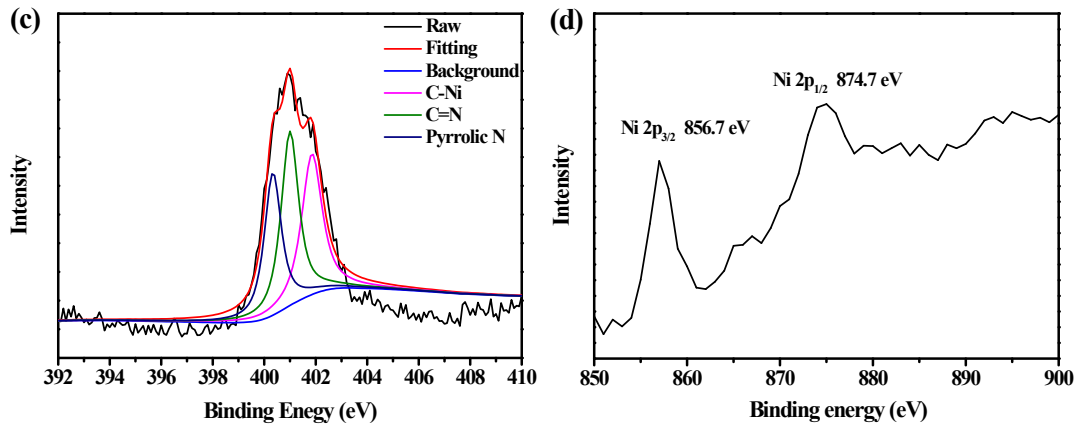


**Figure S3.** (a) Survey scan XPS profiles of PD-COF-23 and PD-COF-23-Ni, (b) and (c) high resolution N 1s spectra of PD-COF-23 and PD-COF-23-Ni, (d) high resolution Ni 2p XPS profiles of PD-COF-23-Ni

**Porosities and BET surface areas analysis**

Nitrogen sorption was measured at 77.3 K using a Micromeritics ASAP 2020 volumetric adsorption analyzer. The sample was degassed in vacuum at 120 °C for 10 h prior to the adsorption measurement. Pore size distributions of COFs were calculated using nonlocal density functional theory (NL-DFT) model.

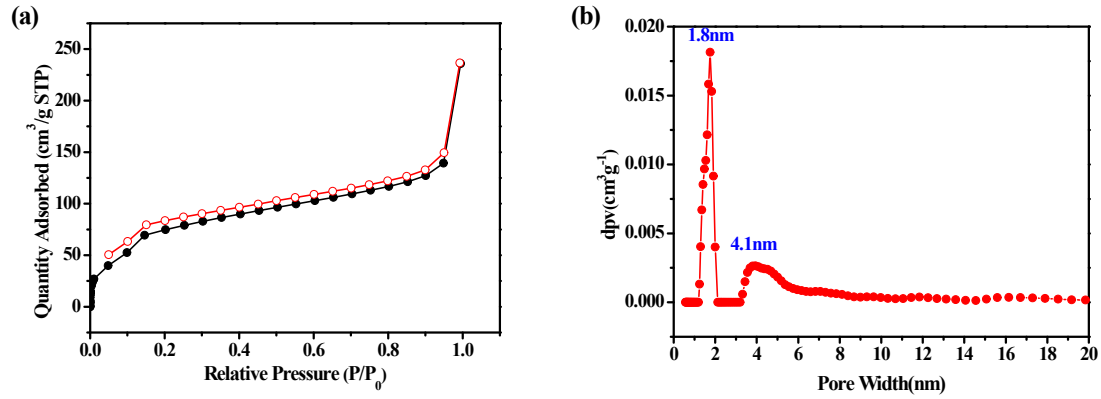

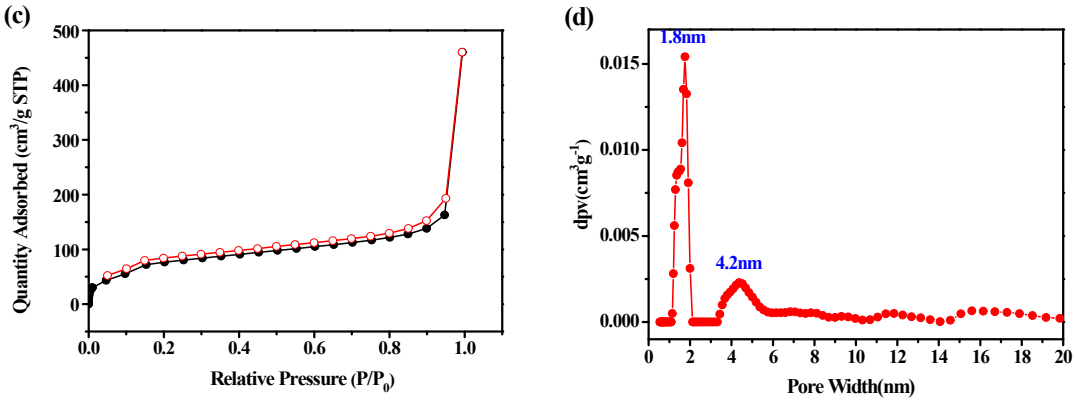


**Figure S4.** Nitrogen sorption isotherm of PD-COF-23 **(a)** and PD-COF-23-Ni **(c)** with pore size distribution **(b)** and **(d)**

## Thermogravimetric analysis

Thermogravimetric analysis (TGA) measurements were performed on Thermogravimetric Analyzer (Perkin Elmer, Norwalk, CT 06859 USA) and the samples were heated from room temperature to 800 °C under nitrogen atmosphere at a heating rate of 10 °C/min.

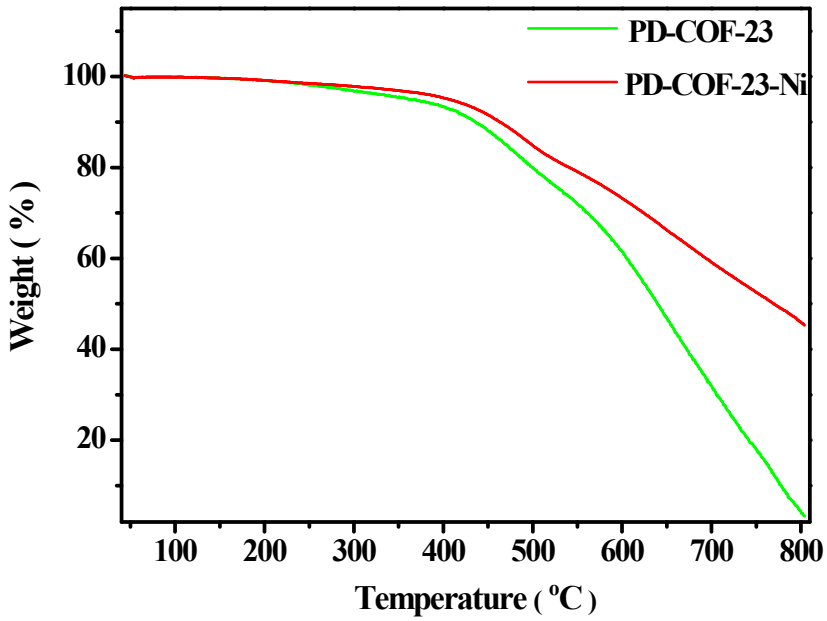


**Figure S5.** TGA curves of PD-COF-23 (green) and PD-COF-23-Ni (red)

## Scanning electron microscopy

The morphology and microstructure of samples were investigated on a field emission scanning electron microscopy (SEM, LEO1530) operated at 20 kV.

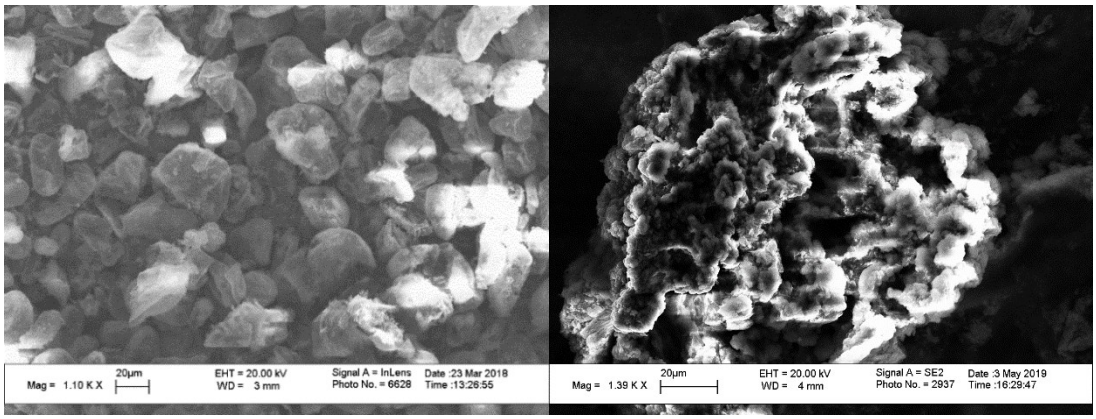


**Figure S6.** SEM of PD-COF-23 (left), PD-COF-23-Ni (right)

**Transmission electron microscopy**

TEM images of the COFs were obtained on transmission electron microscopy (TEM, FEI Tecnai G220) operated at an accelerating voltage of 300 kV.

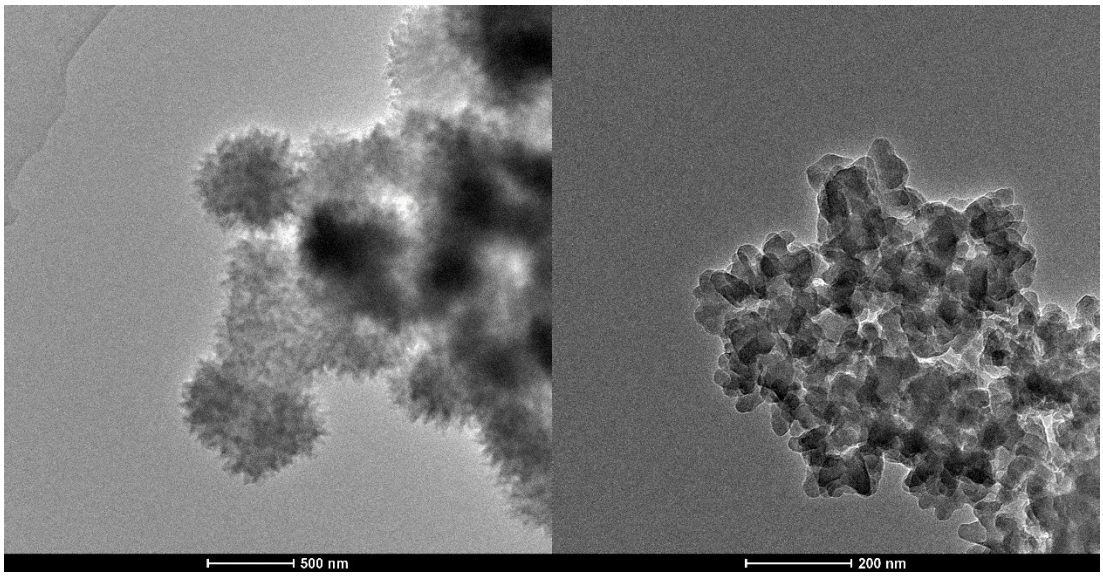


**Figure S7.** TEM of PD-COF-23 (left), PD-COF-23-Ni (right)

## UV-visible absorption spectra

The ultraviolet–visible (UV-Vis) diffuse reflectance spectra (DRS) were obtained by a UV-vis-NIR spectrometer (Perkin Elmer, Lamda 750) equipped with an integrating sphere using $BaSO_4$ as a reference.

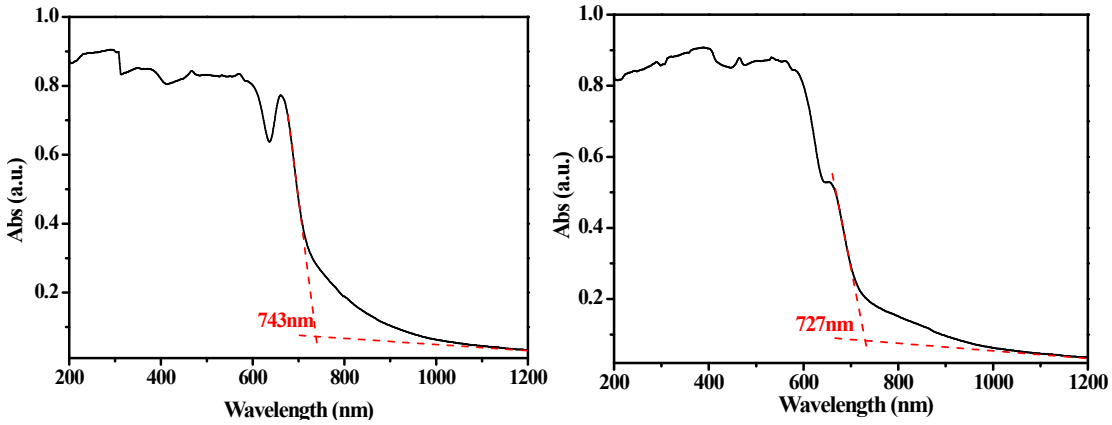


**Figure S8.** UV-vis diffuse reflectance spectra of PD-COF-23 (left) and PD-COF-23-Ni (right)

## Ultraviolet photoelectron spectroscopy

The UPS measurements were conducted with an unfiltered He I gas discharge lamp (21.22 eV).

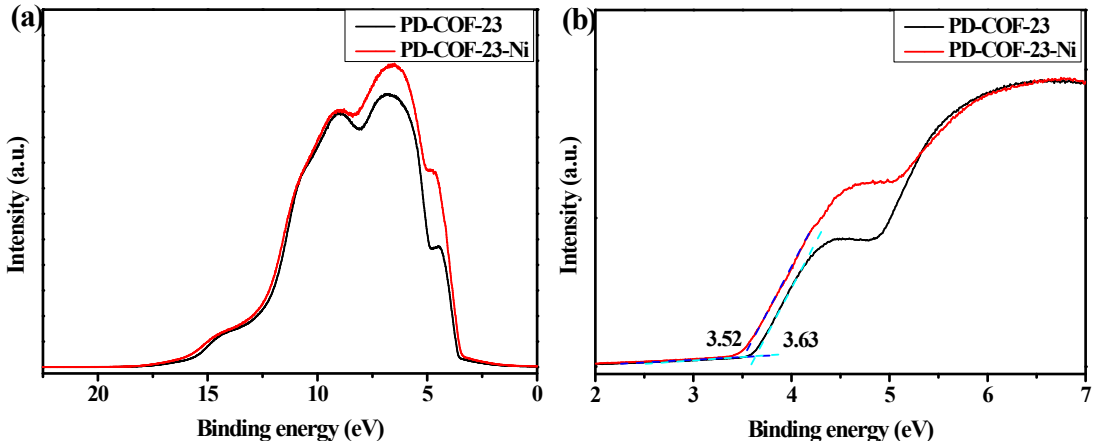

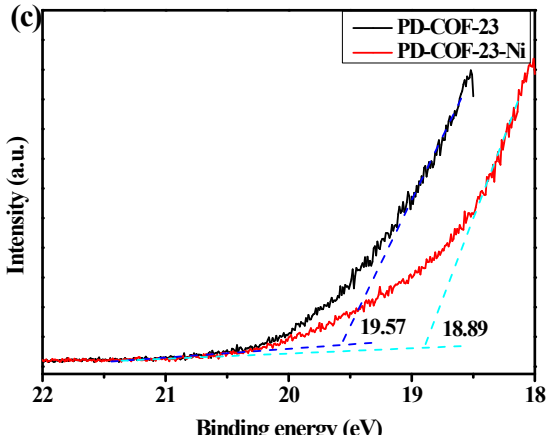


**Figure S9.** UPS spectra of PD-COF-23 and PD-COF-23-Ni: (a) complete spectrum, (b) onset energy region, and (c) cutoff energy region.

## Computational methods

### Structural modeling and PXRD Analysis

Based on the precursor geometries and linking groups the COF structure was constructed, the simulations were carried out with the Materials Studio software 7.0. The X-ray diffraction pattern for the simulated structure was obtained by using the Reflex Powder Diffraction package in the software. Furthermore, Pawley refinement according to the experimental PXRD provided the final unit cell parameters.

Powder X-ray diffraction (PXRD) measurements were carried out on X-ray diffractometer (XRD, Bruker, D8 Advance) with a Cu target in a scanning range of 1.5-50 ° at 0.02 °/min.

**Table S1.** Refined crystal data of PD-COF-23.

| | |
|---|---|
| Space group | C2/m |

| | |
|---|---|
| Crystal system | monoclinic |
| Chemical formula | $C_{200}H_{160}N_{24}O_8$ |
| Unit cell dimension | a = 47.31 Å<br>b = 48.24 Å<br>c = 3.73 Å<br>α = β = 90°<br>γ = 88.46° |

**Table S2.** Fractional atomic coordinates of PD-COF-23.

| Atom | x | y | z |
|---|---|---|---|
| C1 | 0.47856 | 0.55861 | 0.40525 |
| C2 | 0.48636 | 0.58603 | 0.4399 |
| C3 | 0.44465 | 0.52224 | 0.22781 |
| C4 | 0.41949 | 0.51414 | 0.07939 |
| C5 | 0.45158 | 0.55028 | 0.29058 |
| C6 | 0.57111 | 0.57187 | 0.73884 |
| C7 | 0.56519 | 0.59799 | 0.89009 |
| C8 | 0.58595 | 0.61855 | 0.90029 |
| C9 | 0.61333 | 0.6132 | 0.76371 |
| C10 | 0.61964 | 0.5871 | 0.62145 |
| C11 | 0.59872 | 0.56677 | 0.60645 |
| N12 | 0.63468 | 0.6342 | 0.74923 |
| C13 | 0.62944 | 0.6602 | 0.80718 |
| C14 | 0.65189 | 0.68104 | 0.77425 |
| C15 | 0.64457 | 0.70906 | 0.76344 |
| C16 | 0.66543 | 0.72916 | 0.70415 |
| C17 | 0.69394 | 0.72167 | 0.65647 |
| C18 | 0.7011 | 0.69351 | 0.67631 |
| C19 | 0.68031 | 0.67332 | 0.73258 |
| C20 | 0.71468 | 0.74181 | 0.57827 |
| C21 | 0.73546 | 0.78157 | 0.399 |
| C22 | 0.75622 | 0.76193 | 0.44159 |
| O23 | 0.73905 | 0.80515 | 0.29019 |
| N24 | 0.70952 | 0.77044 | 0.48526 |
| C25 | 0.6823 | 0.78366 | 0.426 |
| C26 | 0.67959 | 0.81041 | 0.63736 |

| | | | |
|---|---|---|---|
| C27 | 0.65061 | 0.82277 | 0.58355 |
| C28 | 0.64927 | 0.85141 | 0.74856 |
| H29 | 0.47084 | 0.6032 | 0.37173 |
| H30 | 0.40383 | 0.53044 | -0.0130 |
| H31 | 0.54318 | 0.60265 | 1.00672 |
| H32 | 0.58067 | 0.63973 | 1.0198 |
| H33 | 0.64197 | 0.58231 | 0.51686 |
| H34 | 0.6039 | 0.54562 | 0.48535 |
| H35 | 0.60709 | 0.66718 | 0.88514 |
| H36 | 0.62153 | 0.71557 | 0.80303 |
| H37 | 0.65939 | 0.75202 | 0.69397 |
| H38 | 0.72416 | 0.68684 | 0.64636 |
| H39 | 0.68647 | 0.6505 | 0.74465 |
| H40 | 0.66458 | 0.76894 | 0.51356 |
| H41 | 0.68034 | 0.78856 | 0.12895 |
| H42 | 0.6965 | 0.82567 | 0.53954 |
| H43 | 0.68243 | 0.80593 | 0.93405 |
| H44 | 0.63387 | 0.80897 | 0.71754 |
| H45 | 0.64653 | 0.8243 | 0.28462 |
| H46 | 0.63726 | 0.8504 | 1.01712 |
| H47 | 0.6379 | 0.8661 | 0.56142 |
| H48 | 0.67164 | 0.85931 | 0.79144 |
| N49 | 0.5 | 0.54151 | 0.5 |
| N50 | 0.46055 | 0.5 | 0.31381 |

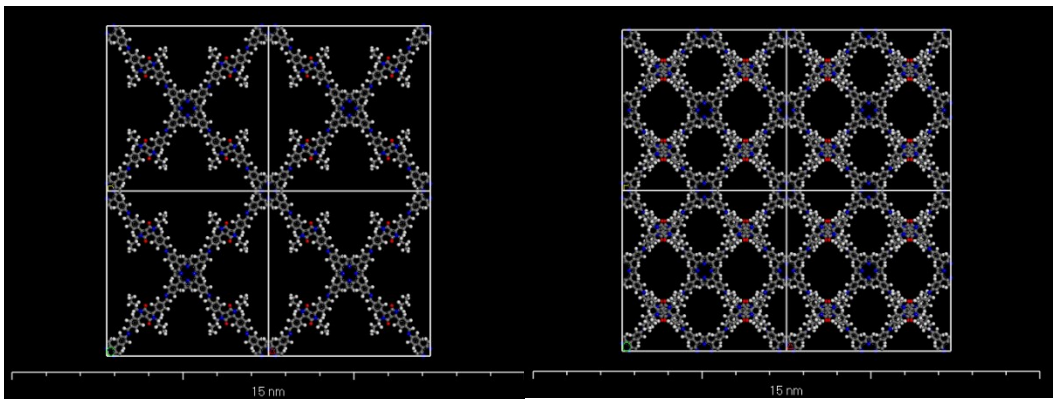


**Figure S10.** Simulation of **PD-COF-23** unit cell calculated in an AA stacking (left) and AB stacking (right) in the *C2/m* space group

**Table S3.** Refined crystal data of PD-COF-23-Ni.

| | |
|---|---|
| Space group | C2/m |

| | |
|---|---|
| Crystal system | monoclinic |
| Chemical formula | $C_{200}H_{160}N_{24}O_8Ni_2$ |
| Unit cell dimension | a = 47.31 Å<br>b = 48.24 Å<br>c = 3.73 Å<br>α = β = 90°<br>γ = 88.46° |

**Table S4.** Fractional atomic coordinates of PD-COF-23-Ni.

| Atom | x | y | z |
|---|---|---|---|
| C1 | 0.47856 | 0.55861 | 0.40525 |
| C2 | 0.48636 | 0.58603 | 0.4399 |
| C3 | 0.44465 | 0.52224 | 0.22781 |
| C4 | 0.41949 | 0.51414 | 0.07939 |
| C5 | 0.45158 | 0.55028 | 0.29058 |
| C6 | 0.57111 | 0.57187 | 0.73884 |
| C7 | 0.56519 | 0.59799 | 0.89009 |
| C8 | 0.58595 | 0.61855 | 0.90029 |
| C9 | 0.61333 | 0.6132 | 0.76371 |
| C10 | 0.61964 | 0.5871 | 0.62145 |
| C11 | 0.59872 | 0.56677 | 0.60645 |
| N12 | 0.63468 | 0.6342 | 0.74923 |
| C13 | 0.62944 | 0.6602 | 0.80718 |
| C14 | 0.65189 | 0.68104 | 0.77425 |
| C15 | 0.64457 | 0.70906 | 0.76344 |
| C16 | 0.66543 | 0.72916 | 0.70415 |
| C17 | 0.69394 | 0.72167 | 0.65647 |
| C18 | 0.7011 | 0.69351 | 0.67631 |
| C19 | 0.68031 | 0.67332 | 0.73258 |
| C20 | 0.71468 | 0.74181 | 0.57827 |
| C21 | 0.73546 | 0.78157 | 0.399 |
| C22 | 0.75622 | 0.76193 | 0.44159 |
| O23 | 0.73905 | 0.80515 | 0.29019 |
| N24 | 0.70952 | 0.77044 | 0.48526 |
| C25 | 0.6823 | 0.78366 | 0.426 |
| C26 | 0.67959 | 0.81041 | 0.63736 |

| | | | |
|---|---|---|---|
| C27 | 0.65061 | 0.82277 | 0.58355 |
| C28 | 0.64927 | 0.85141 | 0.74856 |
| H29 | 0.47084 | 0.6032 | 0.37173 |
| H30 | 0.40383 | 0.53044 | -0.0130 |
| H31 | 0.54318 | 0.60265 | 1.00672 |
| H32 | 0.58067 | 0.63973 | 1.0198 |
| H33 | 0.64197 | 0.58231 | 0.51686 |
| H34 | 0.6039 | 0.54562 | 0.48535 |
| H35 | 0.60709 | 0.66718 | 0.88514 |
| H36 | 0.62153 | 0.71557 | 0.80303 |
| H37 | 0.65939 | 0.75202 | 0.69397 |
| H38 | 0.72416 | 0.68684 | 0.64636 |
| H39 | 0.68647 | 0.6505 | 0.74465 |
| H40 | 0.66458 | 0.76894 | 0.51356 |
| H41 | 0.68034 | 0.78856 | 0.12895 |
| H42 | 0.6965 | 0.82567 | 0.53954 |
| H43 | 0.68243 | 0.80593 | 0.93405 |
| H44 | 0.63387 | 0.80897 | 0.71754 |
| H45 | 0.64653 | 0.8243 | 0.28462 |
| H46 | 0.63726 | 0.8504 | 1.01712 |
| H47 | 0.6379 | 0.8661 | 0.56142 |
| H48 | 0.67164 | 0.85931 | 0.79144 |
| N49 | 0.5 | 0.54151 | 0.5 |
| N50 | 0.46055 | 0.5 | 0.31381 |
| Ni51 | 0.5 | 0.5 | 0.5 |

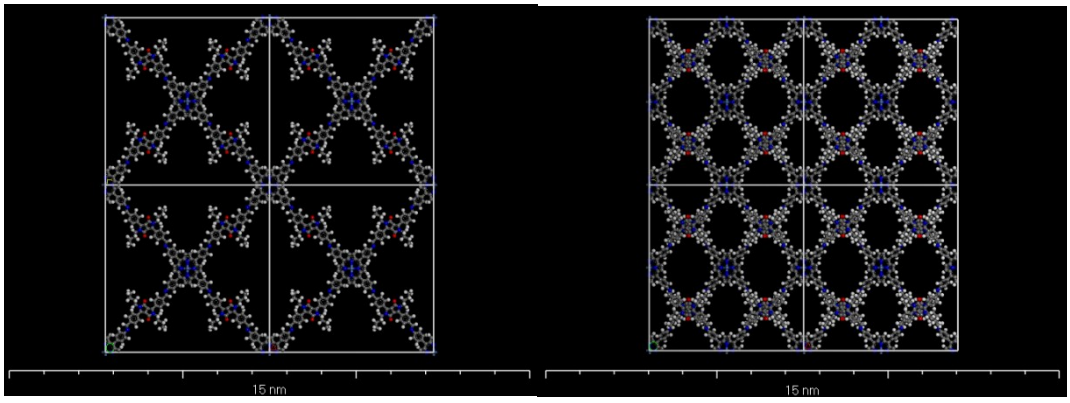


**Figure S11.** Simulation of **PD-COF-23-Ni** unit cell calculated in an AA stacking (left) and AB stacking (right) in the *C2/m* space group

**DFT caculations**

DFT calculations were performed with Gaussian[1] program at PBE0-

D3BJ/def2-SVP level.[2, 3]

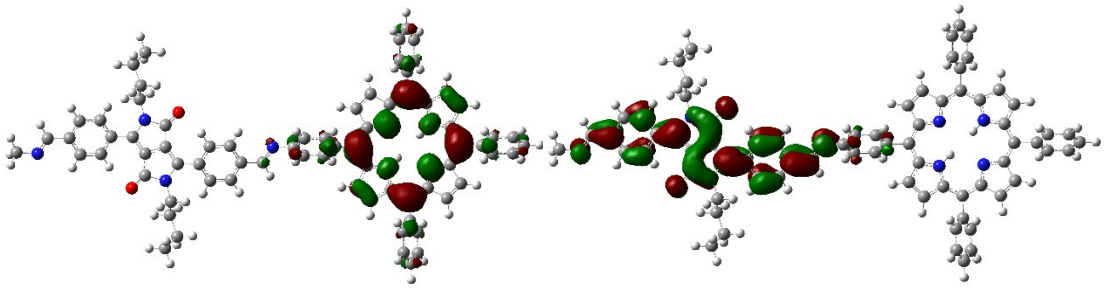

**HOMO** **LOMO**

**Figure S12.** HOMO (left) and LOMO (right) for PD-COF-23 from DFT calculation

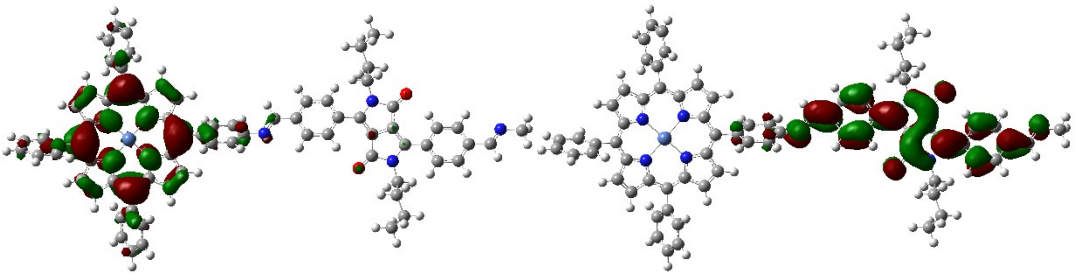

**HOMO** **LOMO**

**Figure S13.** HOMO (left) and LOMO (right) for PD-COF-23 from DFT calculation

## NMR and MALDI-TOF spectrum

### $^{1}$H NMR spectrum

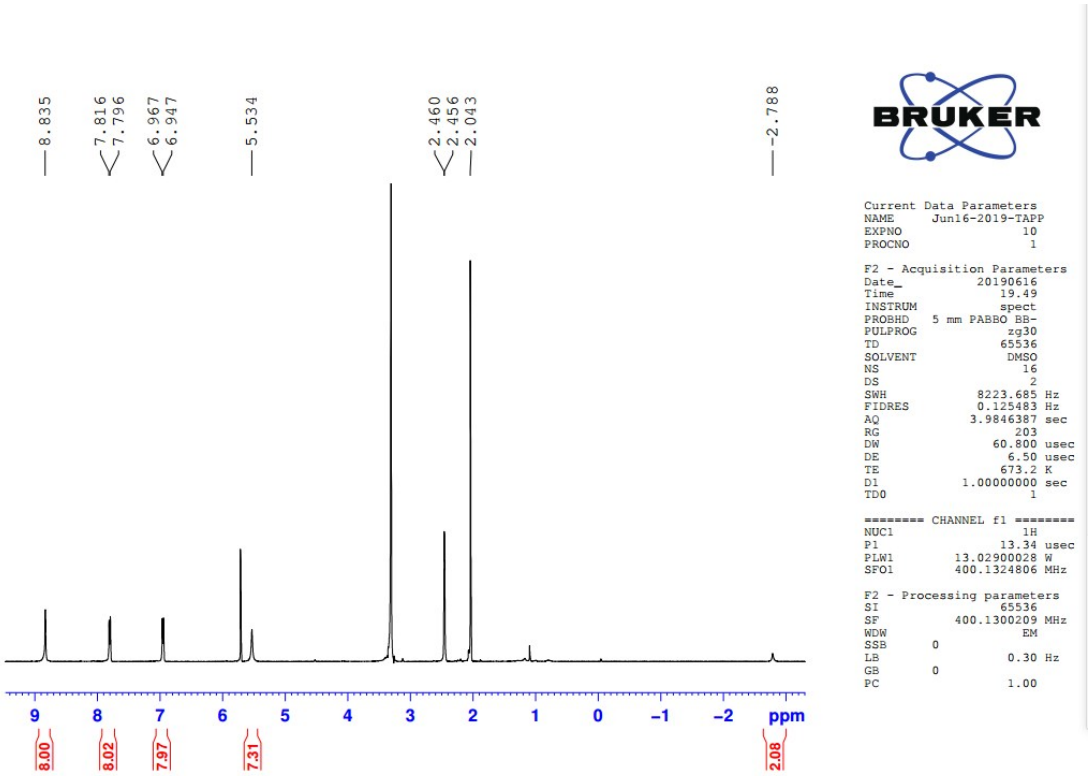


**Figure S14.** [1]H NMR spectra of [1]H NMR spectrum of **TAPP**

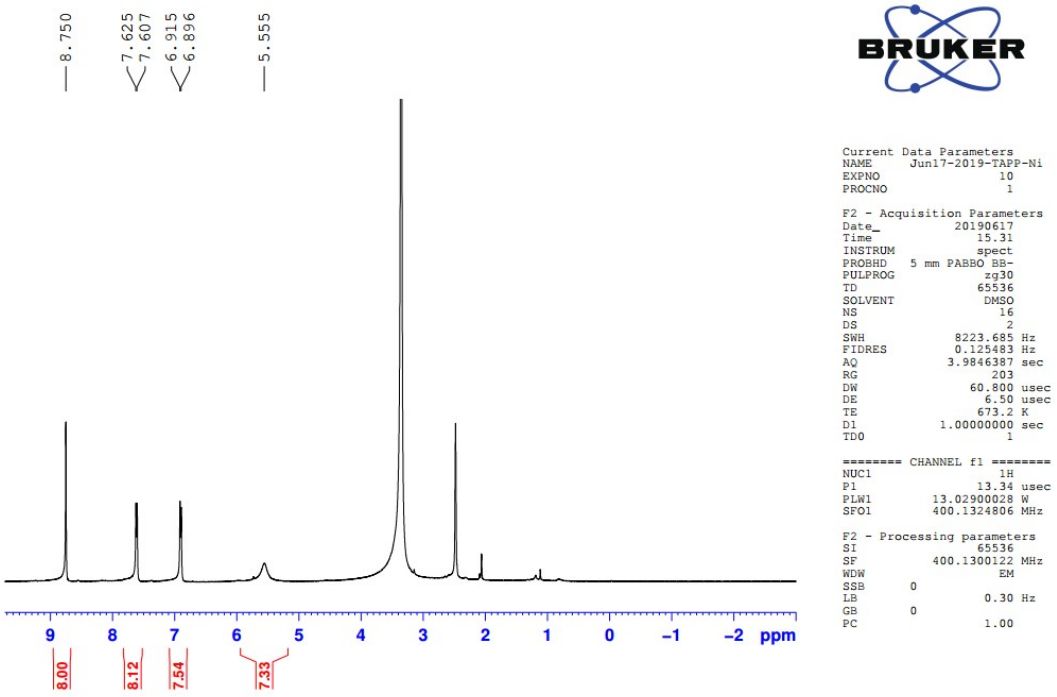


**Figure S15.** [1]H NMR spectrum of **TAPP-Ni**

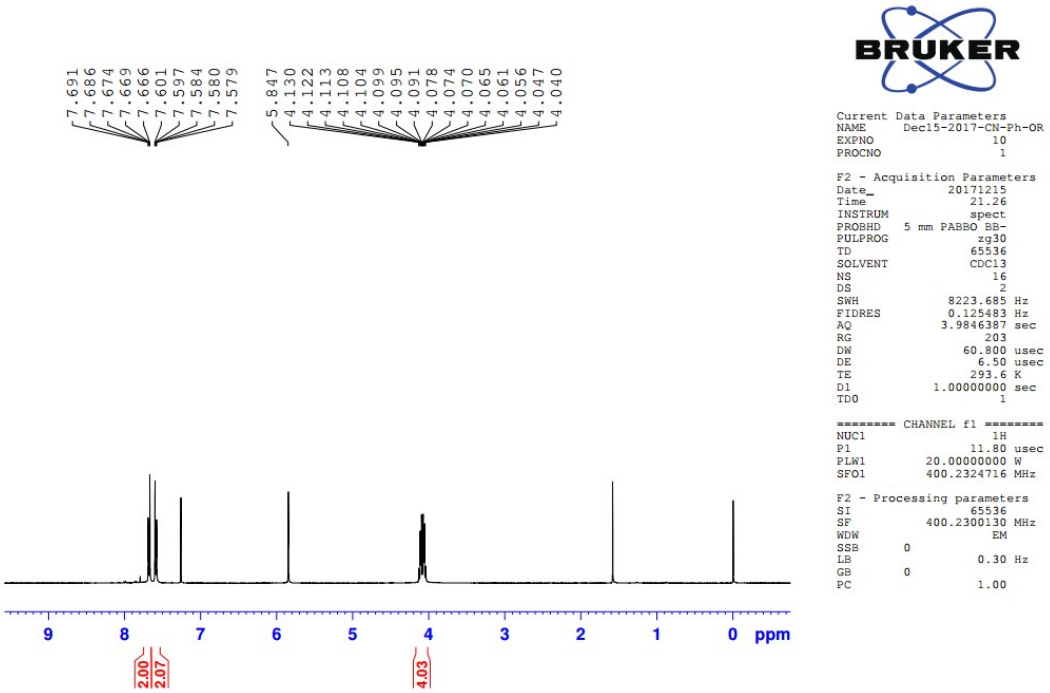


**Figure S16** [1]H NMR spectrum of **S1**

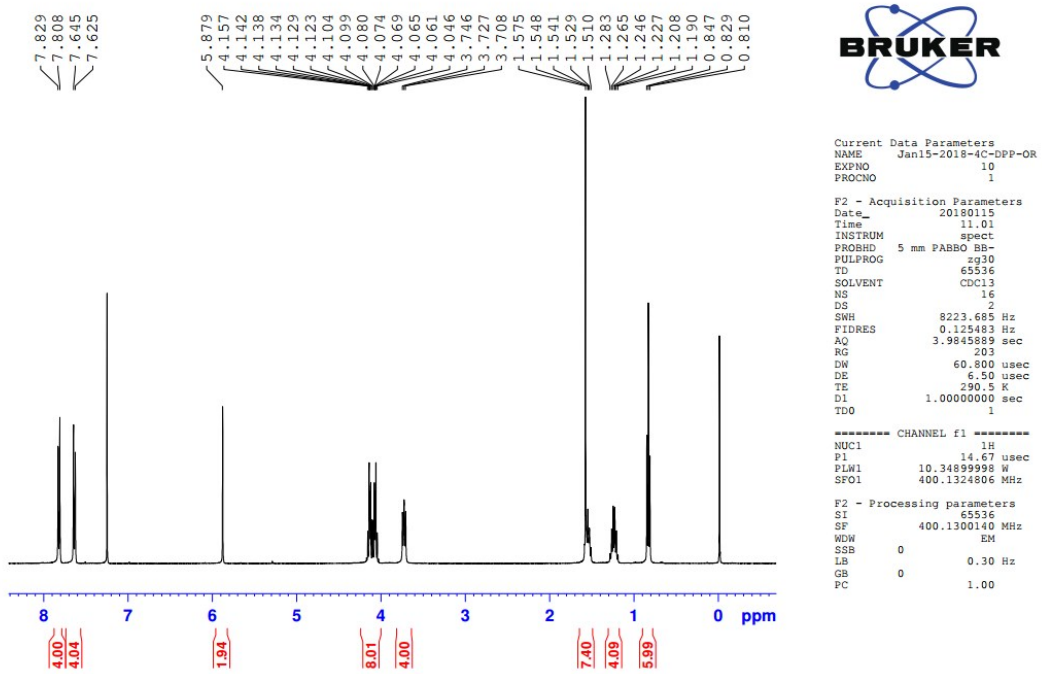


**Figure S17.** [1]H NMR spectrum of **S3**

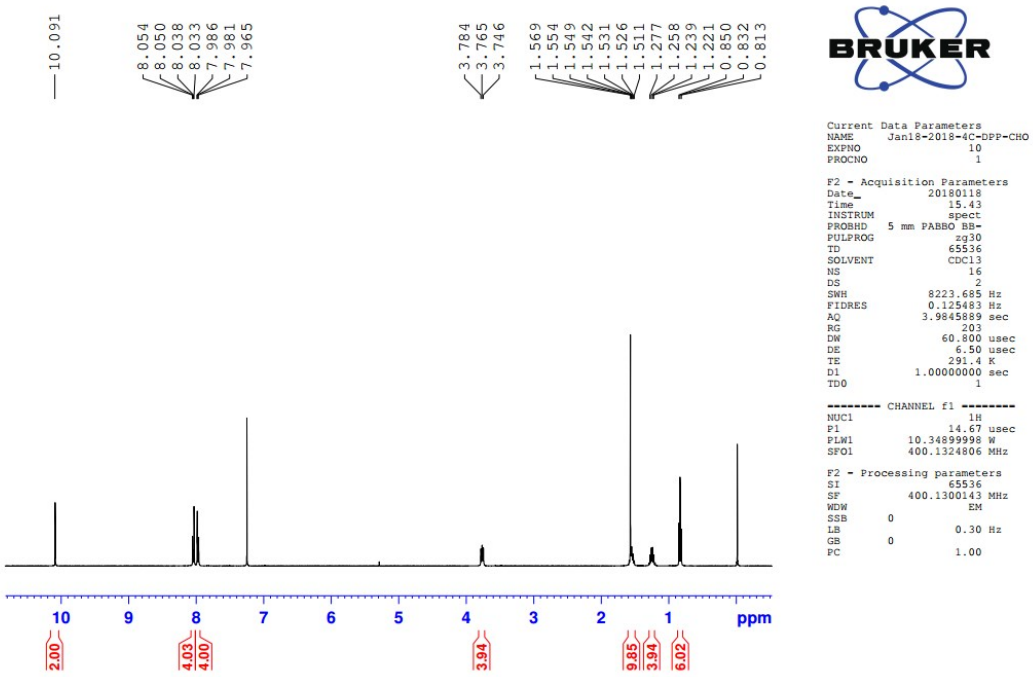


**Figure S18** $^{1}$H NMR spectrm of **DPP-CHO**

## MALDI-TOF spectrum

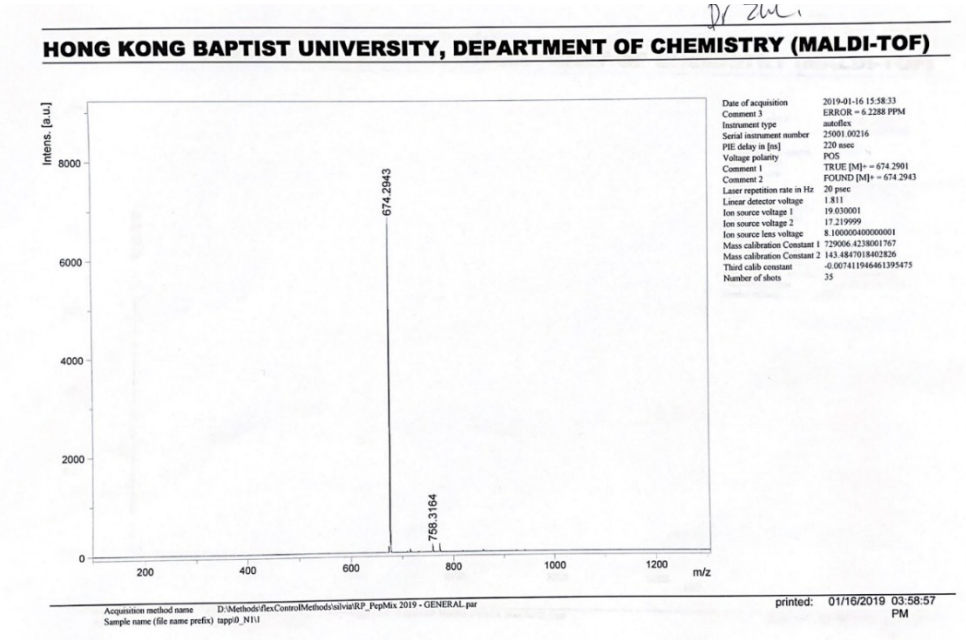


**Figure S19.** Mass spectrum of **TAPP**

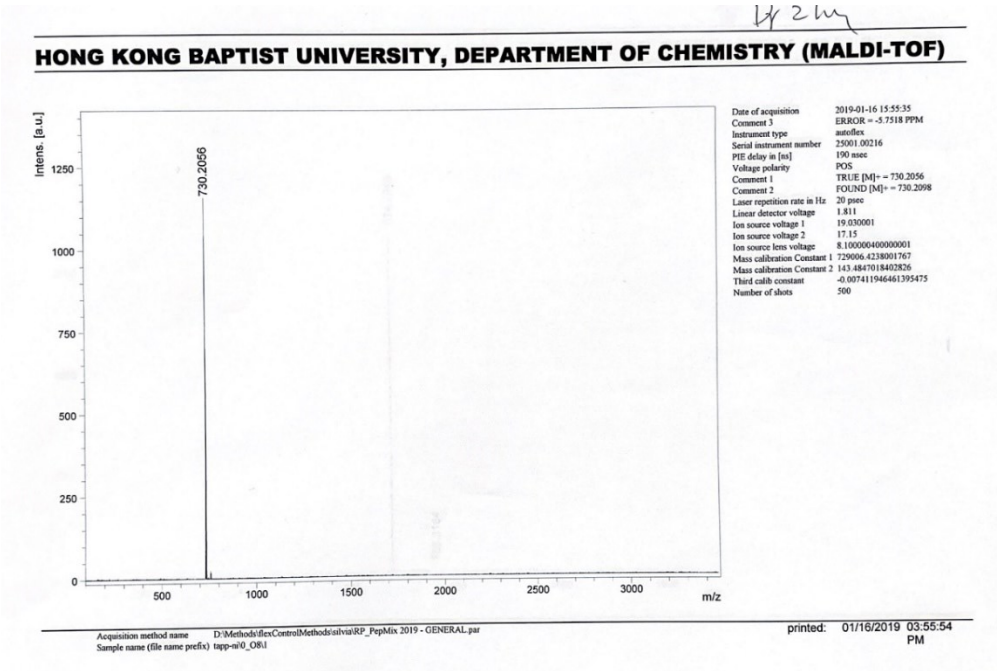


**Figure S20.** Mass spectrum of **TAPP-Ni**

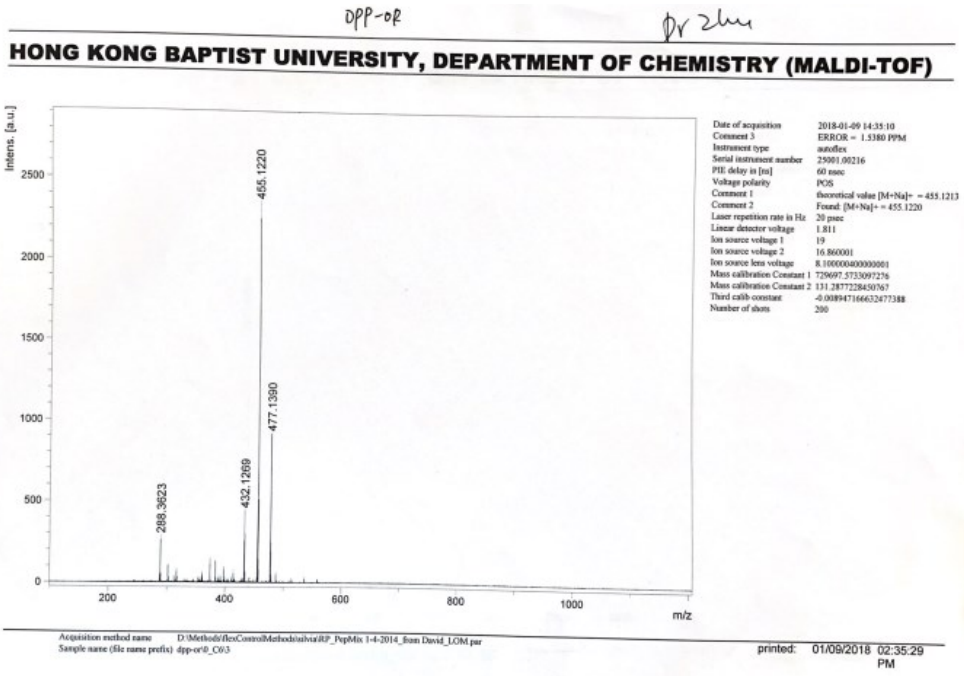

**Figure S21.** Mass spectrum of **S2**

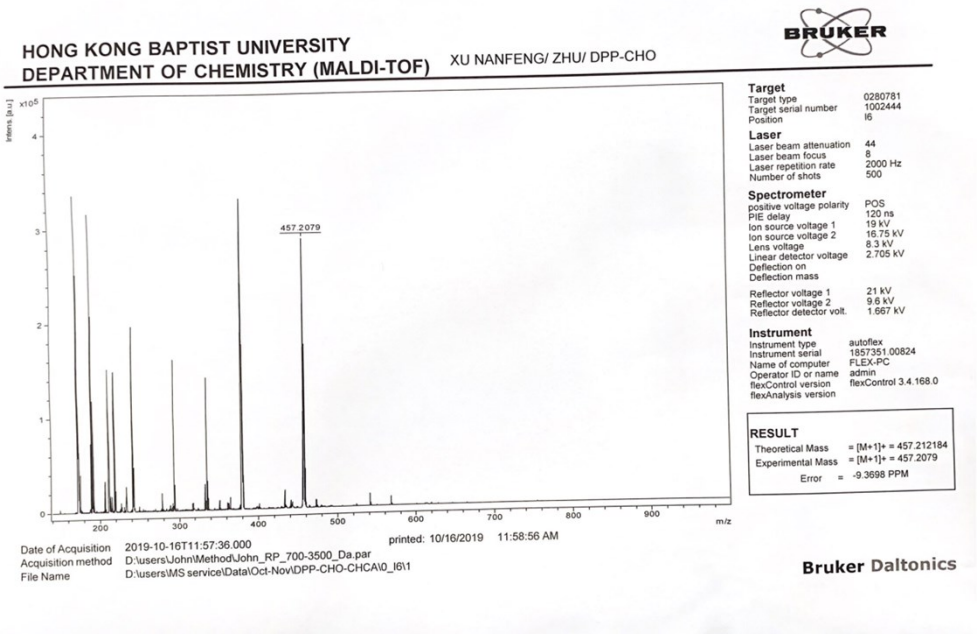


**Figure S22** Mass spectrum of **DPP-CHO**

## Reference

1. X.-Y. Wang, D.-W. Huang, C.-G. Niu, L.-J. Guo, J.-J. Cui, L.-Y. Hu and G.-M. Zeng, *Sensors and Actuators B: Chemical*, 2016, **234**, 593-601.

2. C. Adamo and V. Barone, *J Chem Phys*, 1999, **110**, 6158-6170.

3. S. Grimme, J. Antony, S. Ehrlich and H. Krieg, *J Chem Phys*, 2010, **132**, 154104.